GeoConvention 2014 FOCUS
adapt refine sustain

Time-reversal extrapolation for microseismic event localization

Zhenhua Li, University of Alberta, Canada
zhenhua3@ualberta.ca
and
Mirko van der Baan, University of Alberta, Canada

Summary

Microseismic event localization is important for microseismic monitoring. Travel-time based and migration based methods are used for microseismic event localization. Traveltime based methods require P- and S- wave first arrival picking before further processing. This type of method does not work well for low quality data because of inaccurate arrival picking. Migration based methods avoid picking first arrivals by backpropagating the recorded field to the source location using the velocity model. Time-reversal extrapolation is a typical migration based method. Traditional time-reversal extrapolation is related to adjoint method. We use a representation theorem based extrapolation method to combine the pressure wavefield with its spatial gradient. We then illustrate the method on synthetic borehole data with a limited aperture.

Introduction

Microseismic source imaging is an important technology in microseismic monitoring. The hydraulic fracture process results in microseismic emissions. Microseismic records are used to locate microseismic events and determine source type (Maxwell, 2009). Different event locations indicate the fracture development, and moment tensors reveal the type of failure.

Time reversal extrapolation is a typical migration based extrapolation method, similar to reverse time migration (RTM) (McMechan, 1983, Whitemore, 1983, Baysal et al:, 1983). Traditional time reversal extrapolation is an adjoint state related method (Taratola, 1984) in which a finite difference operator is used for extrapolation (Fleury and Vasconcelos, 2013). Alternatively, acoustic time-reversal extrapolation can be achieved by combining the pressure wavefield and its spatial gradient on the enclosed boundary (Fink, 1999). In the following sections, we first introduce the theory of representation theorem based inverse time extrapolation. Next we show an acoustic example.

Theory and/or Method

The acoustic Representation Theorem can be derived from the first order acoustic wave equations, following the De Hoop (1998), using

$$\oint_{\partial D} \boldsymbol{n}\cdot(\hat{P}^A\hat{\boldsymbol{v}}^B - \hat{P}^B\hat{\boldsymbol{v}}^A)dl = \int_D \hat{\boldsymbol{f}}^A\cdot\hat{\boldsymbol{v}}^B - \hat{\boldsymbol{f}}^B\cdot\hat{\boldsymbol{v}}^A + \hat{q}^B\hat{P}^A - \hat{q}^A\hat{P}^B dS. \qquad (1)$$

where hat ^ indicates a frequency-domain variable, P represents the pressure field of state A/B, ρ represents medium density, v denotes particle velocity of state A/B. f and q are the volume source of force and injection rate respectively. State here simply means a combination of material parameters, field quantities, source distributions, boundary conditions and initial conditions that satisfy the relevant wave equations (van Manen et al., 2006a). Equation (1) is usually called convolution type of representation theorem. It is used for forward extrapolation.

For back extrapolation, we usually use correlation type of representation theorem by time-reversing the wavefield of one state, to get

$$\oint_{\partial D} \boldsymbol{n} \cdot (\hat{P}^{A*}\hat{\boldsymbol{v}}^{B} + \hat{P}^{B}\hat{\boldsymbol{v}}^{A*})dl = \int_{D} \hat{\boldsymbol{f}}^{A*} \cdot \hat{\boldsymbol{v}}^{B} + \hat{\boldsymbol{f}}^{B} \cdot \hat{\boldsymbol{v}}^{A*} + \hat{q}^{B}\hat{P}^{A*} + \hat{q}^{A*}\hat{P}^{B} dS. \tag{2}$$

where conjugate in frequency domain represents time reversal in time domain. Then by assuming one state as the Green's state, we will get the time-reversal extrapolation formula, given by

$$\hat{P}^{*}(\boldsymbol{r}^{B}, \boldsymbol{r}^{A}) + \oint_{D} \hat{G}(\boldsymbol{r}^{B}, \boldsymbol{r})\hat{q}^{*} dS = \oint_{\partial D} \boldsymbol{n} \cdot (\hat{G}(\boldsymbol{r}^{B}, \boldsymbol{r})\frac{1}{i\omega\rho}\boldsymbol{\nabla}\hat{P}^{*}(\boldsymbol{r}, \boldsymbol{r}^{A}) + \hat{P}^{*}(\boldsymbol{r}, \boldsymbol{r}^{A})\frac{1}{i\omega\rho}\boldsymbol{\nabla}\hat{G}(\boldsymbol{r}^{B}, \boldsymbol{r}))dl, \tag{3}$$

We can see that both the pressure wavefield and its spatial gradient on the boundary are combined to back extrapolate the wavefield to the source location. For the acoustic case, the spatial gradient of the pressure wavefield is proportional to the particle velocity.

Example

To better understand the method, we create an infinite homogeneous model with velocity of 3000 m/s. The velocity model is shown in Figure 1. The receivers are in a deviated borehole, as denoted by the upside-down triangles, while the source is explosive modeled with a Ricker wavelet with a peak frequency of 30HZ. Both the pressure and particle velocities in the horizontal and vertical directions are measured in each receiver.

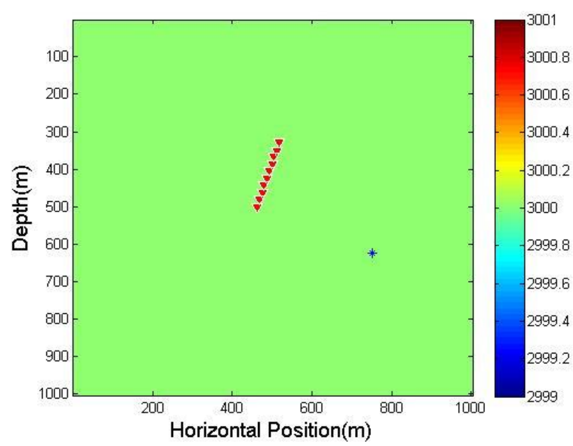

Figure 1 Homogeneous velocity model. Blue cross represents explosive monopole source. Red upside-down triangles represent receivers, which measure pressure and the particle velocities in the horizontal and vertical directions.

Recorded data are spatially sparse and noise contaminated, so we add white noise to the synthetic pressure data and both particle velocities. The signal-to-noise ratio is 0.5. The data are shown in Figure 2, which are highly noise contaminated. The microseismic event is barely visible between 0.125s to 0.17s, highlighted by the red boxes.

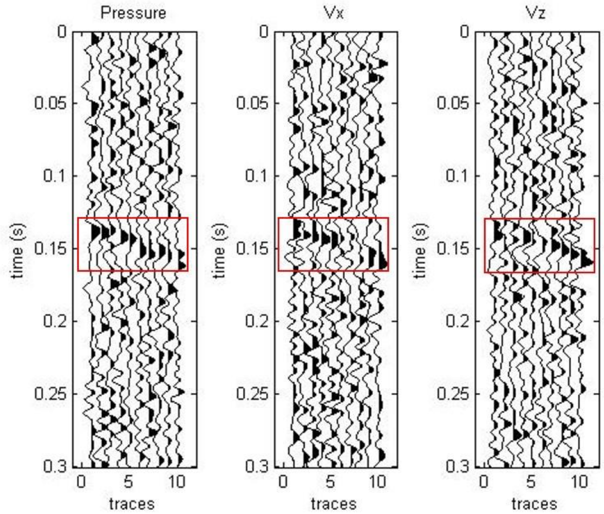

Figure 2 Synthetic data for the homogeneous model including pressure field and two components of the particle velocity field. Data are noise contaminated and sparsely sampled in space. Microseismic event highlighted by the red boxes.

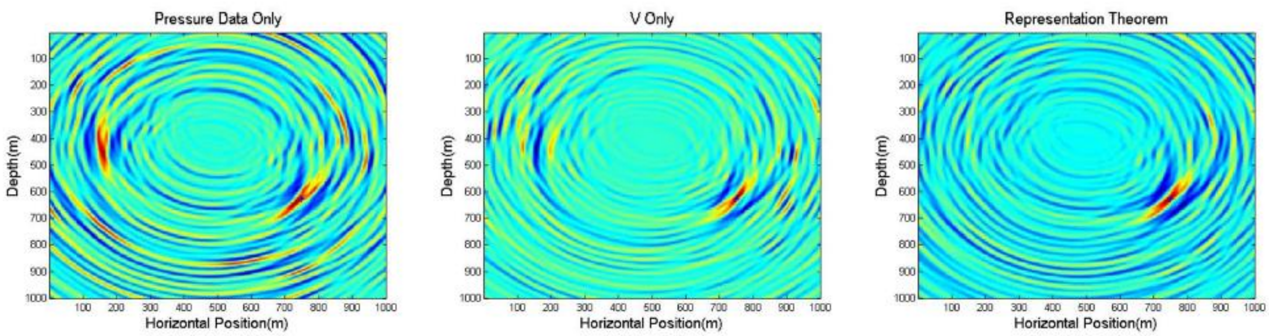

Figure 3 Comparison of three data combinations. Left panel: pressure wavefield only; middle panel: particle velocity wavefields only; right panel : pressure field and both particle velocities. The ghost locations exist in the first two cases, while energy focuses only at true source location when combining all data.

Figure 3 shows the comparison of the back extrapolation results when we apply three different combinations of the total field. The collapsed source location is not perfectly focused because of artifacts from noise and the limited borehole aperture. It can be seen that when we only use pressure field (left), there are two points denoted by two circles in the figure. One is the true source location whereas the other one is ghost location focusing. There is no way to distinguish between them because they have the same phase and similar energy. A similar phenomenon happens when we use both components of the particle velocity field without the pressure wavefield (middle). We find again two possible source locations but with opposite polarities. When we combine all three fields, the ghost image disappears and only the true source location remains. Also, noise artifacts are more suppressed than for the former cases. The true location is easily recognized as it has the peak focusing amplitude.

Conclusions

In this abstract, we introduce a new migration based microseismic event localization method. Representation-theorem-based time-reversal extrapolation offers much promise for obtaining microseismic event locations without the need to first pick individual arrivals, in particular if both the pressure wavefield and its spatial gradients are available. Future investigations will focus on more realistic elastic representation-theorem-based time-reversal extrapolation.

Acknowledgements

The author would like to thank the sponsors of the Microseismic Industry Consortium for financial support.

References

Baysal, E., D. D. Kosloff and J.W. C. Sherwood, 1983, Reverse time migration: Geophysics, 48, 1514-1524.

De Hoop A. T., 1988, Time-domain reciprocity theorems for acoustic wave fields in fluids with relaxation, J. Acoust. Soc. Am., 84(5), 1877-1882.

Fink, M, 1999, Time-reversed acoustics: Scientific American, 91-97.

Fleury, C. and I. Vasconcelos, 2013, Adjoint-state reverse time migration of 4C data: Finite-frequency map migration for marine seismic imaging: Geophysics, 78, no. 2, WA159-WA172.

Maxwell, S., 2009, Assessing the Impact of Microseismic Location Unv=certainties On Interpreted Fracture Geometries: 2009 SPE Annual Technical Conference and Exhibition.

McMechan, G. A., 1983, Migration by extrapolation of time-dependent boundary values: Geophysical Prospecting, 31, 413-420.

Tarantola, A., 1984, Inversion of seismic reflection data in the acoustic approximation: Geophysics, 49, 1259 - 1266.

van Manen, D.-J., A. Curtis and J. O. A. Robertsson, 2006a, Interferometric modeling of wave propagation in inhomogeneous elastic media using time reversal and reciprocity: Geophysics, 71(4), SI47-SI60.